EASR

Engineering and Applied Science Research

https://www.tci-thaijo.org/index.php/easr/index

Published by the Faculty of Engineering, Khon Kaen University, Thailand

Mechanical and thermophysical analysis of B2 structured ferromagnetic materials

Anurag Singh*[1, 2] and Devraj Singh[1]

[1]Department of Physics, Prof. Rajendra Singh (Rajju Bhaiya) Institute of Physical Sciences for Study and Research, VBS Purvanchal University, Jaunpur-222003, India
[2]Department of Physics, Dr. Shyama Prasad Mukherjee Government Degree College, Sant Ravidas Nagar, Bhadohi-221401, India

Received 6 November 2023
Revised 26 March 2024
Accepted 16 May 2024

Abstract

The temperature dependent thermophysical, mechanical and ultrasonic properties of B2 structured ferromagnetic materials MTi (M: Fe, Co, Ni) have been evaluated in present study. The Coulomb and Born-Mayer potential model has been applied to calculate second and third order elastic constants in the temperature range 0-300K. The values of second order elastic constants have been used to find the mechanical and thermophysical properties. The chosen materials have been found ductile as the value of Pugh's indicator for MTi has been found greater than 1.75. The FeTi has been found more stable than CoTi and NiTi. The mechanical constants have been found highest for FeTi. Again, the values of elastic stiffness constants have been used to compute the ultrasonic velocities, Debye average velocities, Debye temperatures, thermal conductivities and Grüneisen parameters along <100>, <110> and <111> directions for the longitudinal and shear modes of wave propagation. The ultrasonic velocities have been observed more for longitudinal mode than shear mode. The ultrasonic velocities and Debye temperatures are found to be highest along <100> direction for all chosen materials. Hence <100> direction would be most suitable for the wave propagation in case of MTi. The obtained values of elastic, mechanical, thermophysical and ultrasonic properties have been compared with existing literatures and discussed.

Keywords: Elastic properties, Mechanical properties, Debye velocity, Grüneisen parameter

1. Introduction

The attractive properties of the alloys of ferromagnetic materials (Fe, Co, Ni), such as hardness, stiffness, corrosion resistance, ductility, electrical and magnetic properties have provided sound base for modern science and technology as wide spread use in electrical and electronic devices. To explore more applications like construction of electrical, electronic, magnetic and memory storage devices for the industrial purposes the alloys of ferromagnetic materials have been drawing great attention among researchers. To increase effectiveness, the alloys of Fe, Co, Ni with IV group elements is one of the most promising areas of study and research for the scientist and engineers [1-6]. The thermodynamic characterizations of ferromagnetic materials at different temperatures are required for technologies and fields of their industrial applications. Zhang et al. [1] investigated influence of applied pressure on the structure, mechanics, dislocation and electronic properties of a ferrotitanium (FeTi) hydrogen storage alloy using first principle computation. They found that FeTi alloy exhibits good mechanical stability in the pressure range 0-50 GPa and also found that FeTi has metallic property structure stability at high pressure. Wollmershauser et al. [2] conducted research on tensile and compression test for CoTi and CoZr for the confirmation of ductile nature of the materials at room temperature. They also noticed that the initial strain hardening rate is exceedingly high. The tensile deformation and fracture mode of hot-rolled CoTi intermetallic has been studied by Kaneno et al. [3]. They perceived that a stoichiometric mixture polycrystalline CoTi has been successfully rolled at 1273K. They also defined brittle-ductile temperature limit for B2 structured CoTi. A self-consistent computation of the electronic structure for (100) surface of B2 structure MTi (M: Fe, Co, Ni) alloys has been presented by Koroteev et al. [4]. They noticed that all the occupied surface states are localized at the surface atoms of the heavier components (Fe, Co and Ni) while all the empty ones are mainly associated with the Ti atoms. Bihlmayer et al. [5] explored the elastic constants of high temperature phases of shape memory alloys (SMAs) NiTi and PdTi by means of full-potential linearized-plane wave total energy computation. They explain the transformation behaviour of SMAs for formation of the martensitic phases. NiTi exhibits shape-memory effect *i.e.*, it changes its shape at low temperature and regain its original shape on heating. Brill et al. [6] performed measurements on the elastic constants of SMA NiTi in the temperature range 100-500K using the ultrasonic technique. Haskins and Lowson [7] determined temperature-dependent mechanical and thermodynamical properties of shape memory alloys NiTi using density functional theory molecular dynamics (DFT-MD). Phase transition of NiTi between B2 and B19' and between B19' and B33 have also been characterized as per the obtained values of thermophysical properties such as thermal energy, entropy and free energy differences as well as the latent heats. Zhu et al. [8] computed pressure dependent structural, elastic, thermodynamic and electronic properties of single crystal B2 structured FeTi using the DFT. They mentioned that the properties of FeTi have been different from the average of the corresponding values found in Fe and Ti. Yu and Liu [9] interrogated the structural, electronic and mechanical properties of B2 structured SMA NiTi at high pressure. They obtained ductile nature of NiTi at high pressure. Matsushita et al. [10] showed the experimental result of direct observation of volume changes and effective thermal

*Corresponding author.
Email address: anuragrajpoot440@gmail.com
doi: 10.14456/easr.2024.43

conductivity measurements of nano-structured FeTi. The porosity and effective thermal conductivity changed due to effect of expansion during hydrogen absorption and contraction during hydrogen desorption, which have been measured simultaneously. Cheng et al. [11] explored the elastic and electronic properties of MTi (M: Fe, Co, Ni) using first principle computation. They found NiTi has most anisotropic behaviour. Pressure dependence on stability and elastic properties of CoTi intermetallic material has been evaluated using first principle calculations with in the generalized gradient approximation (GGA) by Lu et al. [12]. They found that B2 phase of CoTi is most stable as per formation energy analysis. The titanium alloys of ferromagnetic materials have some lucrative properties which makes it very useful than other B2 type materials [13-16]. The procedure for producing FeTi intermetallic material has been demonstrated by Zadorozhnyy et al. [13] by the treatment of Ti 50 at % Fe powder mixture in a high energy ball planetary mill in argon atmosphere. They also discussed the effect of chemical disorder in brief. The equilibrium hydrogen storage properties of nanocrystallines Fe-Ti made by ball milling has been presented by Tessier et al. [14]. Benyelloul et al. [15] examined the influence of hydrogen on the mechanical properties of the intermetallic FeTi and of its FeTiH and $FeTiH_2$ for hydrogen storage applications by the application of density functional theory (DFT) within the generalized gradient approximation (GGA). Padhee et al. [16] reported the mechanistic insights into efficient reversible hydrogen storage in pristine FeTi and Fe_2Ti. They also produced number of thermophysical properties of ferrotitanium like Gibb's free energy and heat capacity.

There are various aspects to enhance the properties of B2 structured ferromagnetic materials for industrial applications to fulfil the increasing demands of present and future. We have surveyed various literatures and found that no work has been done on ultrasonic properties of B2 structured ferromagnetic materials which has motivated us to study the ultrasonic properties with the help of mechanical and thermophysical properties of MTi (M: Fe, Co, Ni) in previous literatures.

Present investigation has been classified into 3 subsections: the theoretical background in Section 2, the results and discussion are presented in section 3; Section 4 includes the conclusion of the investigation.

2. Theory

2.1 Elastic stiffness constants

The second- and third-order elastic constants (SOECs and TOECs) have been computed using Coulomb and Born-Mayer potential for the titanium alloys ferromagnetic materials [17]. In turn SOECs and TOECs are further used to calculate mechanical, thermophysical and ultrasonic properties of the chosen MTi (M: Fe, Co, Ni).

The elastic stiffness constants have defined by [18, 19] as

$$C_{ijklmn=}\partial^n E_n/\partial\eta_{ij}\partial\eta_{kl}\partial\eta_{mn} \tag{1}$$

Where E_n is free energy density and η is Lagrangian strain tensor.

The free energy E_n has defined as

$$E_n = E^s + E^{vib} \tag{2}$$

where E^s is the static part of free energy of the lattice when all ions are at rest and E^{vib} is the vibrational part of free energy. The higher order elastic constants have computed with the help of attractive Coulomb potential ϕ_c and the short range Born-Mayer interaction potential ϕ_b as

$$\phi_c = \pm\frac{e^2}{r} \text{ and } \phi_b = Aexp.\left(-{}^{r}/_{b}\right) \tag{3}$$

Where '*A*' is strength parameter, '*e*' is electrostatic charge, *b* is hardness parameter and '*r*' are nearest neighbour distance.

The second- and third-order elastic constants (SOECs and TOECs) are the sum of static elastic stiffness constants at absolute zero temperature and vibrational energy contribution at particular temperature [19].

$$C_{IJ} = C_{IJ}^S + C_{IJ}^{VIB} \text{ and } C_{IJK} = C_{IJK}^S + C_{IJK}^{VIB} \tag{4}$$

Where the superscript '*S'* stands for the static elastic constant at absolute zero temperature and superscript '*VIB*' indicate the vibrational contribution of elastic constant at required temperature. The expression for the static parts of second- and third-order elastic constants have been obtained [20] as

$$C_{11}^S = \frac{3}{8}\frac{e^2}{r_0^4}S_5^{(2)} + \frac{3\phi(r_1)}{br_0}\left(\frac{\sqrt{3}}{3r_0}+\frac{1}{b}\right) + \frac{2\phi(r_2)}{br_0}\left(\frac{1}{2r_0}+\frac{1}{b}\right)$$

$$C_{12}^S = C_{44}^S = \frac{3}{8}\frac{e^2}{r_0^4}S_5^{(1,1)} + \frac{\phi(r_2)}{br_0}\left(\frac{1}{2r_0}+\frac{1}{b}\right)$$

$$C_{111}^S = -\frac{15}{8}\frac{e^2}{r_0^4}S_7^{(3)} - \frac{\phi(r_1)}{9b}\left(\frac{\sqrt{3}}{r_0^2}+\frac{3}{br_0}+\frac{\sqrt{3}}{b^2}\right) - \frac{\phi(r_2)}{2b}\left(\frac{3}{r_0^2}+\frac{6}{br_0}+\frac{4}{b^2}\right)$$

$$C_{112}^S = C_{166}^S = -\frac{15}{8}\frac{e^2}{r_0^4}S_7^{(2,1)} - \frac{\phi(r_1)}{9b}\left(\frac{\sqrt{3}}{r_0^2}+\frac{3}{br_0}+\frac{\sqrt{3}}{b^2}\right)$$

$$C_{123}^S = C_{456}^S = C_{144}^S = -\frac{15}{8}\frac{e^2}{r_0^4}S_7^{(1,1,1)} - \frac{\phi(r_1)}{9b}\left(\frac{\sqrt{3}}{r_0^2}+\frac{3}{br_0}+\frac{\sqrt{3}}{b^2}\right)$$

Where $S_5^2 = 0.354190$; $S_5^{(1,1)} = 0.346708$; $S_7^{(2,1)} = -0.093356$; $S_7^{(1,1,1)} = -0.159996$; $S_7^3 = 0.540901$; $r_1 = \sqrt{3}r_0$; $r_2 = 2r_0$

$\phi(r_1) = A\exp\left(-\frac{r_1}{b}\right)$; $\phi(r_2) = A\exp\left(-\frac{r_2}{b}\right)$; $A = \frac{bZ_0e^2}{r_0^2}[8\sqrt{3}\,exp\left(\frac{-r_1}{b}\right) + 12exp\left(\frac{-r_2}{b}\right)]$

The expression for the vibrational part of elastic constants has been given in literature [19, 20]

$C_{IJK....}^{VIB} = a_{IJK....}$ T where $a_{IJK.....} = L_1k_B\left|\frac{\partial C_{IJK...}^S}{\partial r}\right|_{r=r_0} + \frac{F_{IJK..}^{VIB}}{TV_C}$

$L_1 = -r_0\left[\frac{8}{3}(2\rho_1 + 2\rho_1^2 - \rho_1^3)\phi(r_1) + \frac{3}{2}(2\rho_2 + 2\rho_2^2 - \rho_2^3)\phi(r_2)\right]Y^{-1}$

$Y = \left[\frac{8}{3}(\rho_1^2 - 2\rho_1)\phi(r_1) + \frac{3}{2}(\rho_2^2 - 2\rho_2)\phi(r_2)\right] \times \left[\frac{8}{3}(\rho_1^2 - 2\rho_1)\phi(r_1) + 2(\rho_2^2 - 2\rho_2)\phi(r_2)\right]$

where $\rho_1 = r_1/b$ and $\rho_2 = r_2/b$

$F_{11}^{VIB} = \frac{k_BT}{4}\left(G_2 - \frac{G_1^2}{6}\right)$; $F_{12}^{VIB} = \frac{k_BT}{4}\left(G_{1,1} - \frac{G_1^2}{6}\right)$; $F_{44}^{VIB} = \frac{k_BT}{4}G_{1,1}$;

$F_{111}^{VIB} = \frac{k_BT}{4}\left(G_3 - \frac{1}{2}G_1G_2 + \frac{G_1^3}{18}\right)$; $F_{112}^{VIB} = \frac{k_BT}{4}\left(G_{2,1} - \frac{1}{3}G_{1,1}G_1 - \frac{1}{6}G_2G_1 + \frac{G_1^3}{18}\right)$;

$F_{123}^{VIB} = \frac{k_BT}{4}\left(G_{1,1,1} - \frac{1}{2}G_1G_{1,1} + \frac{G_1^3}{18}\right)$; $F_{144}^{VIB} = \frac{k_BT}{4}\left(G_{1,1,1} - \frac{1}{2}G_1G_{1,1}\right)$;

$F_{166}^{VIB} = \frac{k_BT}{4}\left(G_{1,1,1} - \frac{1}{2}G_1G_{1,1}\right)$; $F_{456} = \frac{k_BT}{4}G_{1,1,1}$

$G_1 = \left[\frac{8}{9}(2\rho_1 + 2\rho_1^2 - \rho_1^3)\phi(r_1) + \frac{1}{2}(2\rho_2 + 2\rho_2^2 - \rho_2^3)\phi(r_2)\right]Z$;

$G_2 = \left[\frac{8}{27}(-6\rho_1 - 6\rho_1^2 - \rho_1^3 + \rho_1^4)\phi(r_1) + \frac{1}{2}(-6\rho_2 - 6\rho_2^2 - \rho_2^3 + \rho_2^4)\phi(r_2)\right]Z$;

$G_3 = \left[\frac{8}{81}\left(30\rho_1 + 30\rho_1^2 + 9\rho_1^3 - \rho_1^4 - \rho_1^5\right)\phi(r_1) + \frac{1}{2}\left(30\rho_2 + 30\rho_2^2 + 9\rho_2^3 - \rho_2^4 - \rho_2^5\right)\phi(r_2)\right]Z$

$G_{1,1} = \left[\frac{8}{27}(-6\rho_1 - 6\rho_1^2 - \rho_1^3 + \rho_1^4)\phi(r_1)\right]Z$;

$G_{2,1} = G_{1,1,1} = \left[\frac{8}{81}\left(30\rho_1 + 30\rho_1^2 + 9\rho_1^3 - \rho_1^4 - \rho_1^5\right)\phi(r_1)\right]Z$

$Z = \left[\frac{4}{9}(\rho_1^2 - 2\rho_1)\phi(r_1) + \frac{1}{4}(\rho_2^2 - 2\rho_2)\phi(r_2)\right]$

The pressure derivatives of second order elastic constants (PDSOECs) have been calculated using the SOECs and TOECs. PDSOECs for measuring the effect of hydrostatic pressure to crystal symmetry as [19]

$$\left\{\begin{array}{c} \frac{dC_{11}'}{dp} = -\frac{2C_{11}+2C_{12}+C_{111}+2C_{112}}{C_{11}+2C_{12}}\,;\ \frac{dC_{12}'}{dp} = -\frac{-C_{11}-C_{12}+C_{123}+2C_{112}}{C_{11}+2C_{12}}\,; \\ \frac{dC_{44}'}{dp} = -\frac{C_{11}+2C_{12}+C_{44}+C_{144}+2C_{166}}{C_{11}+2C_{12}} \end{array}\right\} \quad (5)$$

2.2 Mechanical constants

Three independent SOECs C_{11}, C_{12}, C_{44} have been used to compute the mechanical parameters like bulk modulus (B_L), shear modulus (G_S), Young modulus (Y_E), Poisson ratio (σ), Zener anisotropy (A_n) and Pugh's indicator (P_G) for MTi at room temperature has been expressed with the following formulae [21].

$$\left\{\begin{array}{c} B_L = \frac{(C_{11}+C_{12})}{2}\,;\ G_S = \frac{(C_{11}-C_{12}+3C_{44})}{10} + 2.5(C_{11}-C_{12})C_{44}; Y_E = \frac{9GB}{(G+3B)}; \\ \sigma = \frac{(3B-2G)}{(6B+2G)}\,; A_n = \frac{2C_{44}}{(C_{11}-C_{12})} \end{array}\right\} \quad (6)$$

2.3 Ultrasonic velocities

The SOECs have been applied to compute ultrasonic velocities for longitudinal and shear modes of propagation along <100>, <110> and <111>. When an ultrasonic wave travels through a nonlinear solid crystalline matter, due to compression effect of lattice atoms three modes of acoustical waves has been generated one longitudinal or compression wave and two shear waves, which depend on direction of propagation and mode of polarization. These three acoustical velocities depend directly on square root of SOECs and inverse square root of the mass density of B2 structured material MTi in following ways [22].

Along <100> direction

$V_L = \sqrt{C_{11}/\rho}$; $V_{S1} = V_{S2} = \sqrt{C_{44}/\rho}$; (7)

Along <111> direction

$V_L = \sqrt{(C_{11} + 2C_{12} + 4C_{44})/3\rho}$; $V_{S1} = V_{S2} = \sqrt{(C_{11} - C_{12} + C_{44})/3\rho}$; (8)

Along <110> direction

$V_L = \sqrt{(C_{11} + C_{12} + 2C_{44})/2\rho}$; $V_{S1} = \sqrt{C_{44}/\rho}$; $V_{S2} = \sqrt{(C_{11} - C_{12})/\rho}$; (9)

With the help of longitudinal and shear velocities, the Debye average velocity (V_D) along different directions has been obtained in the following way.

Along <100> and <111> direction

$$V_D = \left[\frac{1}{3}\left\{\frac{1}{V_L^3} + \frac{2}{V_{S1}^3}\right\}\right]^{-1/3} \quad (10)$$

Along <110> direction

$$V_D = \left[\frac{1}{3}\left\{\frac{1}{V_L^3} + \frac{1}{V_{S1}^3} + \frac{1}{V_{S2}^3}\right\}\right]^{-1/3} \quad (11)$$

2.4 Thermophysical properties

The Debye average velocities have been used to compute the Debye temperature (θ_D) [22] as

$$\theta_D = \frac{h}{k_B}\left(\frac{3nN\rho}{4\pi M}\right)^{1/3} V_D \quad (12)$$

The thermal mechanisms can be explained with the help of Debye temperature which depends on molecular weight (M), density (ρ), Debye average velocity (V_D), number of atoms per unit cell (n), Boltzmann constant (k_B), Avogadro's number (N) and Planck's constant (h).

The thermal conductivity (κ) has been defined as the ability of a material to conduct heat. When acoustical wave has been propagated through a crystalline material it has transported heat to the lattice points and phenomenon of thermal conductivity occurs. κ is expressed by Morelli and Slack's approach [23] as

$$\kappa = \frac{A\bar{M}_a\delta\theta_D^3 \quad n^{1/3}}{\gamma^2 T} \quad (13)$$

Where T is temperature, n is number of atoms per unit cell, δ (in Å) is the cube root of volume per atom, A=3.04×10^{-8}, $\bar{M}_a$is defined as molecular weight in amu. γ^2 has defined as average square of Grüneisen constant. The Grüneisen constant (γ) along different modes <100>, <110> and <111> has been calculated using Mason's approach [24]. The Grüneisen parameters depend on thermal expansion coefficient, specific heat capacity at constant volume and compressibility of crystalline material and are independent of temperature. The specific heat capacity at constant volume (C_v) and energy density (E_0) has obtained using data from $\left(\theta_D/_T\right)$ Tables of AIP Handbook [25].

3. Results and discussion

The second and third order elastic stiffness constants (SOECs and TOECs) of FeTi, CoTi and NiTi have been computed in B2 phase using lattice parameters (r) 2.96 Å, 2.99Å and 3.01 Å respectively [26]. The value of hardness parameters (b) [27] has been taken 0.303Å for all materials. The stiffness constants have calculated with in temperature range 0-300K under the conditions that r and b are independent of temperature. The calculated values of SOECs and TOECs for MTi (M: Fe, Co, Ti) at wide range of temperatures have been presented in Table 1.

Table 1 SOECs and TOECs (all in GPa) for MTi (M: Fe, Co, Ni) in the temperature range 0-300K.

Material	Temp(K)	C_{11}	C_{12}	C_{44}	C_{111}	C_{112}	C_{123}	C_{114}	C_{116}	C_{456}	Ref.
FeTi	0	324.58	185.90	185.90	-1904.6	-98.11	8.71	8.71	-98.11	8.71	Present
	0	385	95	72							[8]
	0	392.02	106.02	65.23							[16]
	0	372.95	87.10	68.63							[26]
	100	321.76	184.03	185.44	-1850.9	-107.3	14.26	14.32	-91.27	10.76	
	200	318.93	182.16	184.99	-1797.1	-116.6	19.81	19.94	-84.42	12.81	
	300	316.10	180.29	184.54	-1743.4	-125.8	25.36	25.55	-77.58	14.86	
CoTi	0	313.25	178.55	178.55	-1840.0	-98.82	3.78	3.78	-98.82	3.78	Present
	0	286.51	113.79	74.66							[26]
	100	310.48	176.73	178. 13	-1786.6	-108.13	9.19	9.47	-91.92	5.82	
	200	307.70	174.91	177.72	-1733.3	-117.45	14.61	15.16	-85.02	7.85	
	300	304.93	173.09	177.30	-1679.9	-126.77	20.02	20.85	-78.13	9.89	
NiTi	0	305.98	173.85	173.85	-1798.5	-99.22	0.68	0.68	-99.22	0.68	Present
	0	195.93	157.59	62.90							[26]
	100	303.24	172.06	173.46	-1745.4	-108.60	6.00	6.42	-92.29	2.71	
	200	300.50	170.28	173.06	-1692.3	-117.99	11.33	12.16	-85.34	4.74	
	300	297.76	168.49	172.67	-1639.1	-127.37	16.65	17.90	-78.43	6.76	

From Table 1 it has been clear that the values of elastic stiffness constants change with varying temperature. The values of C_{12} and C_{44} have found to be equal at 0K but decrease on increasing temperature while C_{123}, C_{144} and C_{456} have been found to be equal at

0K as per Cauchy's relation and increase on increasing temperature. C_{111}, C_{112} and C_{166} having negative values predicts that the values of C_{111}, C_{166} increase on decreasing temperature and C_{112} decrease with increase in temperature. The obtained elastic constants from Table 1 follows FeTi > CoTi > NiTi. Thus, it can be said that FeTi is more elastically stable than CoTi and NiTi. The obtained values of the elastic constants have been compared with available results [8, 16, 26] as shown in Table 1. The elastic stability can be determined by satisfying these inequalities [28], $C_{11} + 2C_{12} > 0$, $C_{11} - C_{12} > 0$ and $C_{44} > 0$ for structural stable cubic compounds. The calculated SOECs in present case obey the inequalities of stability criterion which proves that MTi are elastically stable in B2 phase at all temperatures. Under stress free condition at 0K when ions of the crystal lattice are in rest the Cauchy's relations defined by Cousin [29], $C^0_{123} = C^0_{456} = C^0_{144}$; $C^0_{12} = C^0_{44}$; $C^0_{112} = C^0_{166}$ are satisfied. From Table 1 it is obvious that at 0K the Cauchy relations for all chosen B2 structured ferromagnetic materials hold good which indicates that the crystalline ions interact with central force and situated at a centre of inversion. The pressure derivatives of SOECs [30] under elastic nonlinearity conditions have been calculated with Eq. (5). The temperature dependent pressure derivatives of second order elastic constants have been depicted in Figure 1.

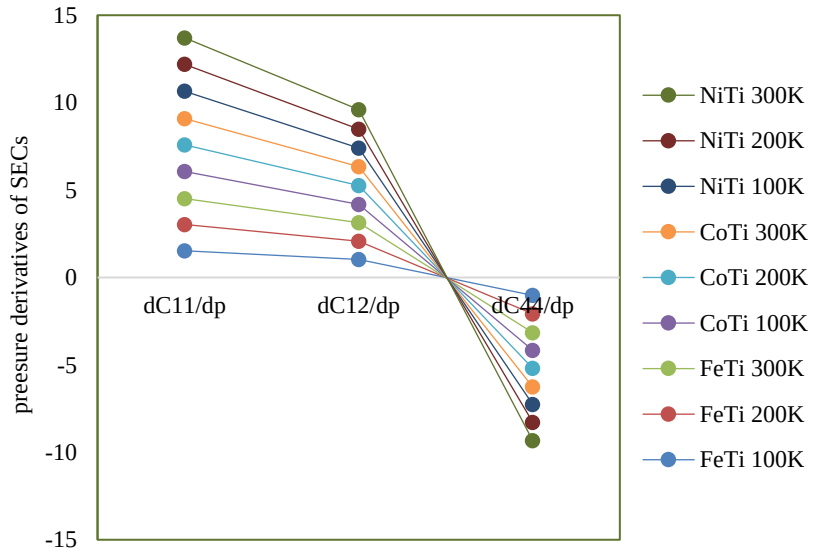

Figure 1 Temperature dependent pressure derivatives of SOECs for FeTi, CoTi and NiTi

A perusal of Figure 1 shows that the pressure derivatives of SOECs decrease with increase in temperature following the order FeTi < CoTi < NiTi. Conservation of crystal symmetry for a CsCl type crystal has been determined by hydrostatic pressure [19]. The Pressure derivatives of C_{11}, and C_{12} are positive while pressure derivatives of C_{44} is negative. From Figure 1 it has been clear that C_{11}, C_{12} and C_{44} are increasing with hydrostatic pressure for B2 structured MTi.

These calculated elastic stiffness constants have been further used to calculate various mechanical parameters as Young modulus (Y_E), bulk modulus (B_L), shear modulus (G_S), Poisson's ratio (σ), Zener anisotropy (A_n) and Pugh indicator (P_G) and have been presented in Table 2.

Table 2 Y_E, B_L, G_S (all in 10^{11} Nm^{-2}), σ, A_n and P_G of MTi (M: Fe, Co, Ni) with in temperature range 0-300K

Material	Temp (K)	Y_E	B_L	G_S	σ	A_n	P_G	Ref.
FeTi	0	31.84	23.21	12.52	0.27	2.68	1.85	Present
	0	23.73	18.24	9.25	0.28		1.97	[26]
	100	31.68	22.99	12.47	0.27	2.69	1.84	
	200	31.52	22.78	12.42	0.27	2.71	1.83	
	300	31.36	25.56	12.36	0.27	2.72	1.83	
CoTi	0	30.55	21.79	12.03	0.27	2.66	1.84	Present
	0	20.57	17.34	7.91	0.29		2.16	[26]
	100	30.55	22.13	12.03	0.27	2.66	1.84	
	200	30.40	21.92	11.98	0.27	2.68	1.83	
	300	30.24	21.70	11.93	0.27	2.69	1.82	
NiTi	0	30.00	21.79	11.80	0.27	2.63	1.85	Present
	0	10.91	16.00	3.91	0.39		4.35	[26]
	100	29.83	21.58	11.75	0.27	2.65	1.84	
	200	29.68	21.37	11.70	0.27	2.66	1.83	
	300	29.52	21.16	11.65	0.27	2.67	1.82	

From Table 2 it has seen that mechanical constants have been found out highest for FeTi and follow the order as FeTi > CoTi > NiTi in B2 phase with in temperature range 0-300K. At 0K the available values of mechanical parameters in [26] are comparable with present values. As shown in Table 2 approximate variation has been found 5% to 25% in computed results. The Young modulus defined as ratio of longitudinal stress to longitudinal strain has related to the stiffness of material. Stiffness of the materials increase with

increasing the values of Young modulus. On increasing temperature, it has been depicted from Table 2 that values of mechanical constants are decreasing. The bulk modulus represents the compressibility of the material. The higher the values of bulk modulus represent that material is highly resistant to fracturing. The bulk modulus for FeTi has been observed to be highest and least for NiTi. It decrease with increase in temperature. The shear modulus represents the hardness of the material and higher the values of shear modulus represent that material is highly resistant to plasticity. The higher values of mechanical constants represent that the materials are harder, stiffer and mechanically stable. From Table 2 it is clear that FeTi is harder and stiffer than CoTi and NiTi at 100K and decay with rise in temperature. NiTi has been found softest material and has low resistance against deformation due to low hardness and stiffness. The Pugh's indicator or fracture to toughness ratio measures the ductility or brittleness of material. For ductility the Pugh's factor [31] should be greater than 1.75 and for brittleness it should be less than 1.75. It can be predicted by Table 2 that the values of P_G are greater than 1.75 for B2 type MTi (M: Fe, Co, Ni) with in temperature range 100-300K, which indicates that all materials under present investigation are ductile. The nature of interatomic force of a solid crystal either central or non-central will be decided by Poisson's ratio. For central forces, the value of Poisson's ratio should be greater than 0.25 but less than 0.5 [32]. In present case the σ value is 0.27, which shows that inter-atomic forces are central for FeTi, CoTi and NiTi for chosen temperature range. The isotropic or anisotropic characteristics of solids have been determined by Zener anisotropic factor (A_n). For isotropic materials its value has unity while for anisotropic materials its value departs from unity. The calculated values of Zener anisotropic factor have been greater than unity, which reveals that chosen materials are anisotropic in nature. The anisotropy plays a crucial role in determination of phase transformation, deformation to plasticity, fracture and toughness etc.

The three modes of ultrasonic velocities $(V_L,\ V_{S1}, V_{S2})$ have been computed at different temperatures and along different directions using Eqs. (7-9). The obtained results of ultrasonic velocities $(V_L,\ V_{S1}, V_{S2})$ have been presented in Table 3. These ultrasonic velocities have further used to calculate Debye average velocity (V_D) using Eqs. (10-11) and are presented in Table 3.

Table 3 Temperature dependent V_L, V_{S1}, V_{S2}, V_D (all in ms^{-1}) along <100>, <110> and <111>.

Material	Temperature(K)	Direction	V_L	V_{S1}	V_{S2}	V_D
FeTi	100	<100>	6.96	5.29	5.29	5.66
		<110>	8.13	5.29	3.22	4.27
		<111>	8.48	4.03	4.03	4.53
	200	<100>	6.93	5.28	5.28	5.65
		<110>	8.10	5.28	3.21	4.26
		<111>	8.45	4.02	4.02	4.52
	300	<100>	6.90	5.27	5.27	5.64
		<110>	8.07	5.27	3.20	4.24
		<111>	8.43	4.01	4.01	4.51
CoTi	100	<100>	6.84	5.18	5.18	5.56
		<110>	7.97	3.96	3.18	4.20
		<111>	8.32	5.18	3.96	4.45
	200	<100>	6.81	5.17	5.17	5.55
		<110>	7.95	5.17	3.16	4.19
		<111>	8.29	3.95	3.95	4.44
	300	<100>	6.78	5.17	5.17	5.54
		<110>	7.92	5.17	3.15	4.18
		<111>	8.27	3.94	3.94	4.43
NiTi	100	<100>	6.84	5.17	5.17	5.45
		<110>	7.96	5.17	3.18	4.21
		<111>	8.30	3.96	3.96	4.45
	200	<100>	6.81	5.17	5.17	5.54
		<110>	7.94	5.17	3.17	4.19
		<111>	8.28	3.95	3.95	4.44
	300	<100>	6.78	5.16	5.16	5.53
		<110>	7.91	5.16	3.16	4.18
		<111>	8.25	3.94	3.94	4.43

Table 3 clears it, that ultrasonic velocities have been varying with temperature as these velocities decrease with temperature and increase from <100> to <111>. The ultrasonic velocities follow the order FeTi > CoTi > NiTi. The longitudinal mode of acoustical velocities for MTi (M: Fe, Co, Ni) have highest value along <111>, while lowest along <100>. The longitudinal velocity is higher than shear velocity, which shows that vibration of lattice points due to compressional motion is higher than transverse motion of wave. The Debye velocities have found to be maximum for MTi at 100K and along <100> direction and decrease from CoTi to NiTi. The Debye average velocities have found minimum at 300K along <110> direction for MTi (Y: Fe, Co, Ni). The calculated values of ultrasonic velocities have compared with available values in literature [26] and we have found that for FeTi, CoTi and NiTi V_L=7.87×10^{3}ms^{-1}, 7.38×10^3 ms^{-1}, 6.83×10^3 ms^{-1} V_S=4.41×10^3 ms^{-1}, 3.95×10^3 ms^{-1}, 3.03×10^3 ms^{-1} ; V_D =4.90×10^3 ms^{-1}, 4.41×10^3 ms^{-1}, 3.41×10^{3}ms^{-1} and θ_D =352K, 314K and 241K respectively. The highest mode of vibration can be achieved by Debye temperature which correlates the elastic properties with thermal properties. The Debye temperature has been obtained using Eq. (12). The achieved results of Debye temperature have been visualized in Figure 2 for MTi along <100>, <110> and <111> directions.

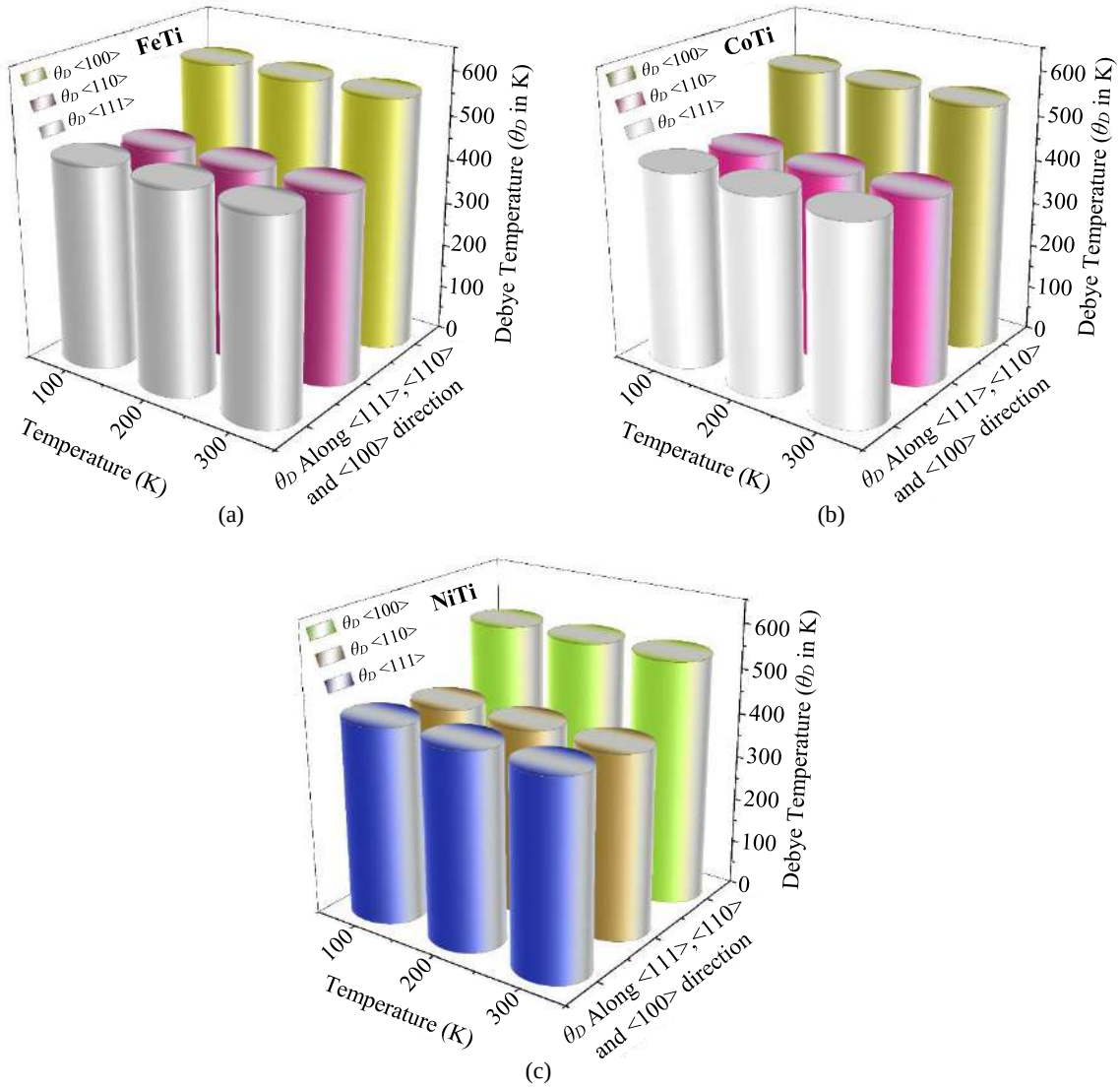

Figure 2 The Debye temperature for (a) FeTi, (b) CoTi, (c) NiTi at 100-300K along <100>, <110> and <111> directions.

It is clear from Figure 2 that the Debye temperature is highest along <100> and lowest along <110> for all selected B2 structured MTi. The Debye temperature has slight decreasing trend from FeTi to NiTi within temperature 100K to 300K because θ_D directly depends on density and Debye velocity while inversely depends on molecular weight. The temperature dependent thermal conductivity (κ) phenomenon arises due to transportation of heat from one lattice point to another due to phonon vibration. The thermal conductivity depends on molecular weight and Debye temperature while inversely proportional to the temperature. The thermal conductivity (κ) has been calculated using Eq. (13) and presented in Figure 3 for FeTi, CoTi and NiTi along <100>, <110> and <111> directions.

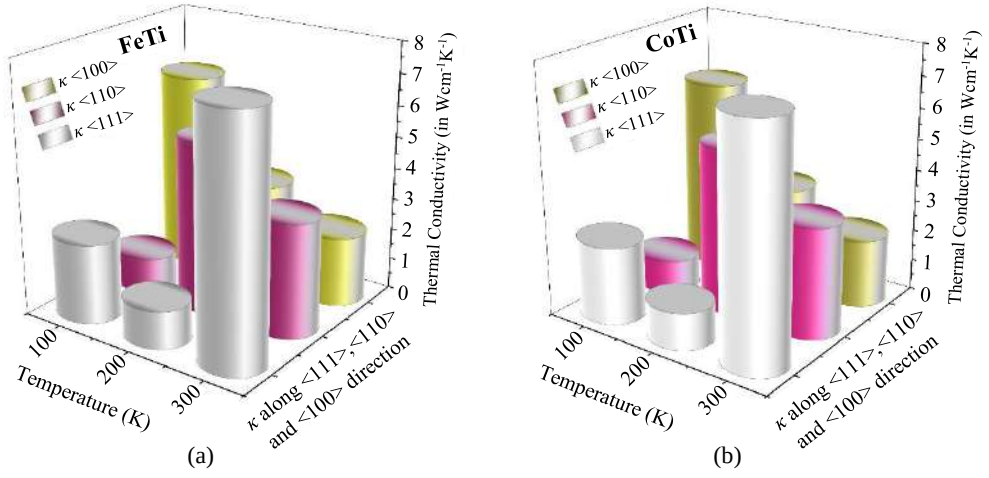

Figure 3 The thermal conductivity (κ) for (a) FeTi, (b) CoTi, (c) NiTi in the temperature range 100-300K along < 100 >, < 110 > and < 111 > direction.

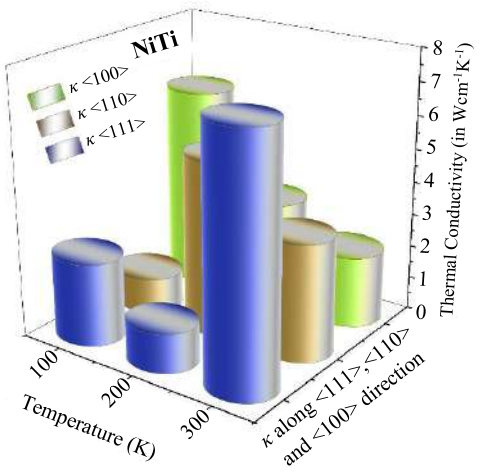

(c)

Figure 3 (continued) The thermal conductivity (κ) for (a) FeTi, (b) CoTi, (c) NiTi in the temperature range 100-300K along < 100 >, < 110 > and < 111 > direction.

From Figure 3, the highest value of thermal conductivities has been found at 300K along <111> while lowest value at 100K along <110> for FeTi, CoTi and NiTi. Thus better thermal purpose could be attained at 300K along <111> direction. The thermal conductivities could be explained on the basis of deviation number ΔN which varies from 0-4. The deviation number ΔN has been defined as the difference of the column number of first element (M) and second element (Ti) of B2 structured MTi in the helical periodic table [33]. The thermal conductivity has highest value for ΔN=0 and decrease on increasing ΔN. For B2 type FeTi, CoTi and NiTi the value of ΔN has been found to be equal to 4 which shows that B2 structured ferromagnetic materials have very low order of thermal conductivity. The ultrasonic Grüneisen parameters have calculated with the help of SOECs and TOECs using Mason's theory and presented in Table 4.

Table 4 The Grüneisen parameters $\langle \gamma_i^j \rangle$ and square average of Grüneisen parameters $\langle (\gamma_i^j)^2 \rangle$ along <100>, <110> and <111> directions for temperature range 100-300K.

Material	Temp (K)	Direction	$\langle \gamma_i^j \rangle_L$	$\langle (\gamma_i^j)^2 \rangle_L$	$\langle (\gamma_i^j)^2 \rangle_{S1}$	$\langle (\gamma_i^j)^2 \rangle_{S2}$
FeTi	100	<100>	-0.1012	0.1890	0.1286	0.1286
		<110>	0.0719	0.4681	0.9603	0.3658
		<111>	0.1587	0.2486	0.2820	0.2820
	200	<100>	-0.1069	0.1829	0.1310	0.1310
		<110>	0.0719	0.4681	0.9425	0.3266
		<111>	0.1587	0.2486	0.2519	0.2519
	300	<100>	-0.1126	0.1777	0.1336	0.1336
		<110>	0.0844	0.4603	0.9254	0.2900
		<111>	0.1678	0.2589	0.2241	0.2241
CoTi	100	<100>	-0.0981	0.1846	0.1247	0.1247
		<110>	0.0557	0.4700	1.0247	0.3595
		<111>	0.1463	0.2330	0.2760	0.2760
	200	<100>	-0.1040	0.1784	0.1272	0.1272
		<110>	0.0685	0.4611	1.0030	0.3196
		<111>	0.1556	0.2429	0.2455	0.2455
	300	<100>	-0.1100	0.1732	0.1298	0.1298
		<110>	0.0815	0.4535	0.9823	0.2825
		<111>	0.1651	0.2536	0.2174	0.2174
NiTi	100	<100>	-0.0960	0.1817	0.1222	0.1222
		<110>	0.0532	0.4653	1.0719	0.3553
		<111>	0.1440	0.2290	0.2721	0.2721
	200	<100>	-0.1021	0.1754	0.1247	0.1247
		<110>	0.0663	0.4565	1.0472	0.3150
		<111>	0.1536	0.2391	0.2413	0.2413
	300	<100>	-0.1082	0.1702	0.1273	0.1273
		<110>	0.0796	0.4490	1.0235	0.2776
		<111>	0.1634	0.2501	0.2130	0.2130

A relation between thermal expansion coefficient, compressibility and specific heat capacity could be established with the help of ultrasonic Grüneisen parameter. The Grüneisen parameter $\langle \gamma_i^j \rangle$, responsible for anharmonicity of lattice, has been calculated with the help of second- and third-order elastic constants for longitudinal and shear modes along <100>, <110> and <111> orientations [34], where 'i' stands for mode and 'j' stands for direction of propagation. UGPs have been found highest along <100> for chosen MTi. The square average of shear UGPs have been observed dominant over longitudinal UGPs. The transverse wave propagation for square average of UGPs have found to be highest along <110> direction and polarized along <1$\bar{1}$0>. There has not existed any theoretical or experimental results of Grüneisen constant for direct comparison so the obtained values have been compared with similar B2 structured materials [21, 22, 34] which validated our theoretical approach. The specific heat capacity per unit volume (C_V) and energy density (E_0) have obtained using AIP Handbook and are presented in Figure 4 and Figure 5 respectively.

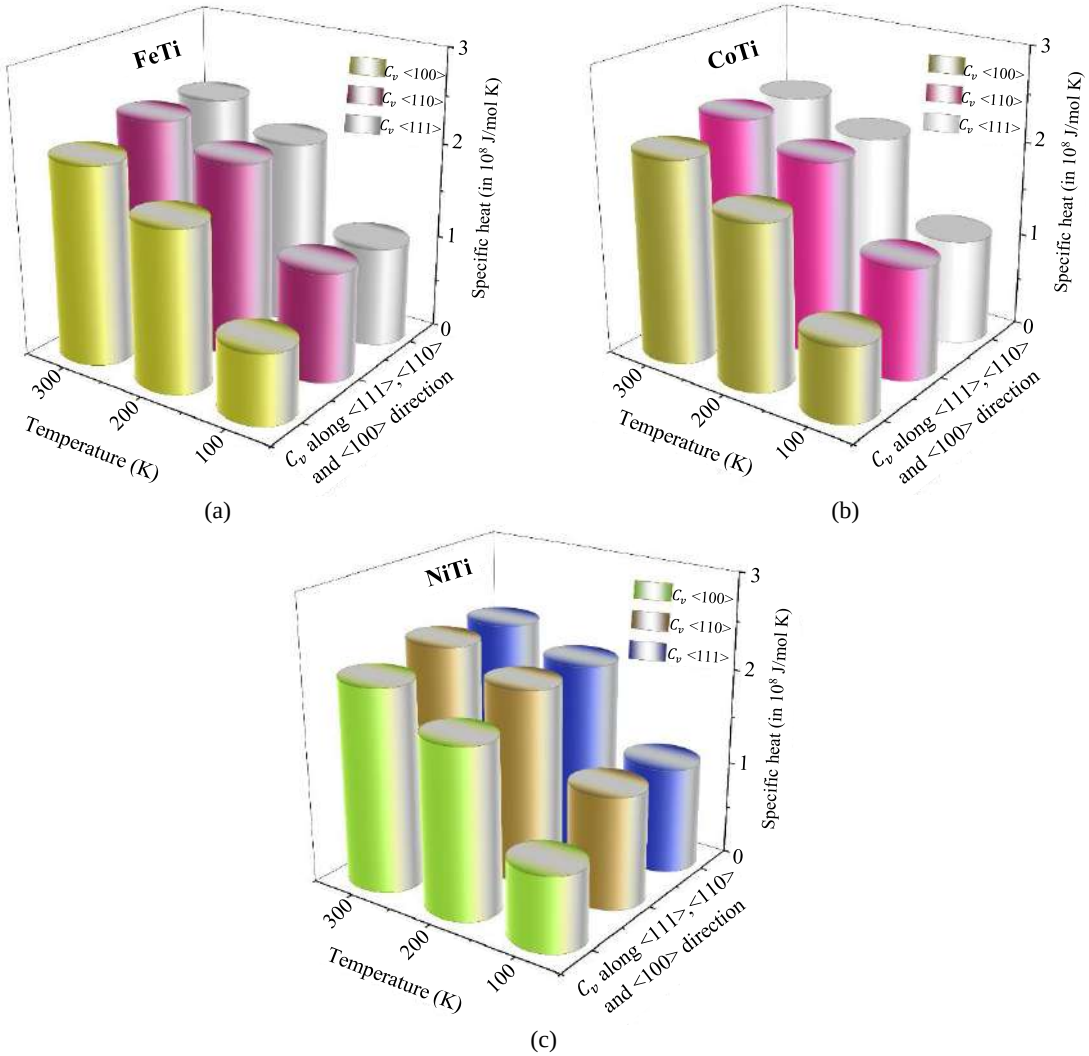

Figure 4 The specific heat capacity per unit volume for (a) FeTi, (b) CoTi, (c) NiTi in temperature range 100-300K along < 100 >, < 110 > and < 111 > direction.

The specific heat capacity per unit volume (C_v) and energy density (E_0) have been found to be increasing with temperature. From Figure 4 we have seen that values of C_v are highest along <110> and lowest along <100> for MTi at all chosen temperatures. The values of C_v at 300K and along <110> have been found nearly equal. When we compare among materials individually, we found from Figure 4 that C_v is maximum for NiTi and lowest for FeTi along <100>, <110>, <111> at temperature range 100-300K. Variation of Energy density E_0 for MTi at different temperatures along different directions has been shown in Figure 5.

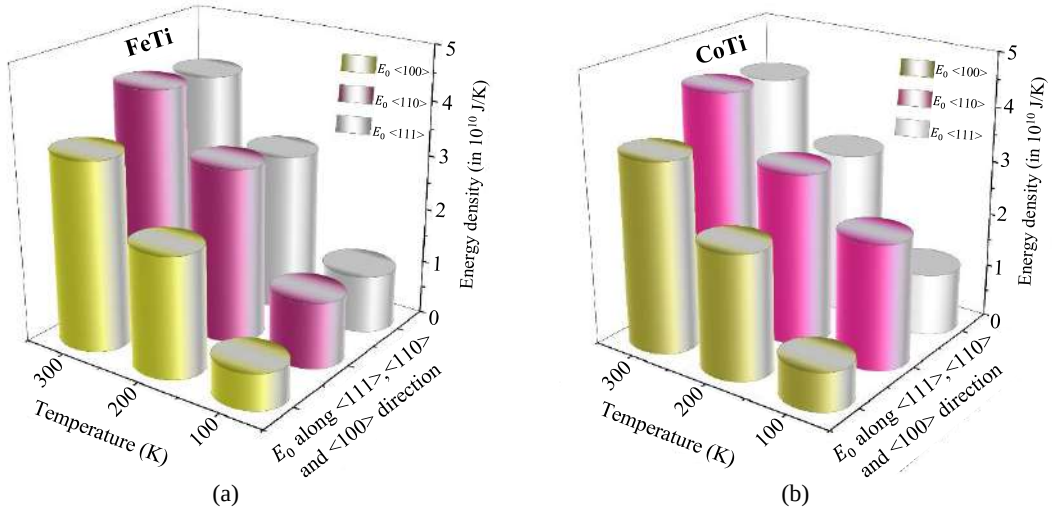

Figure 5 The energy density for (a) FeTi, (b) CoTi, (c) NiTi in temperature range 100-300K along < 100 >, < 110 > and < 111 > direction.

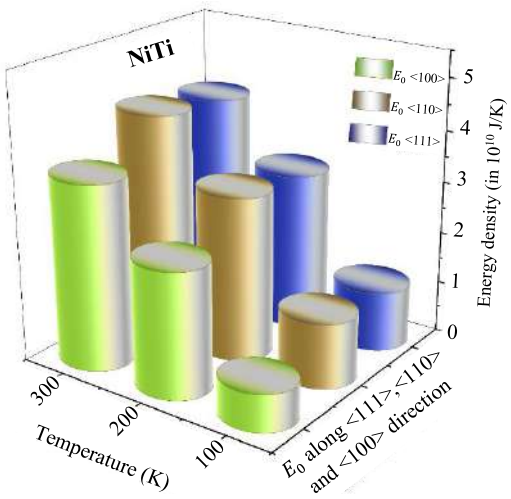

(c)

Figure 5 (continued) The energy density for (a) FeTi, (b) CoTi, (c) NiTi in temperature range 100-300K along < 100 >, < 110 > and < 111 > direction.

Figure 5 depicts that energy densities follow the order NiTi > CoTi > FeTi. E_0 have been found to be highest for NiTi at 300K along <110> direction and lowest for FeTi at 100K along <110> direction. The nature of E_0 has been found comparable with available similar type of materials [21, 22, 34].

4. Conclusion

Using the Coulomb and Born-Mayer potential model, the second- and third-order elastic constants have investigated for MTi (M: Fe, Co, Ni) in the temperature range 0-300K. Resemblance of our results with preceding previous calculations show that our method to compute elastic constants is decent and authentic. The investigated materials MTi are stable and ductile. The ultrasonic velocities of FeTi are highest along <100> direction with in the temperature range 100-300K. So <100> direction is most appropriate for propagation of ultrasonic wave. The Debye temperatures and thermal conductivities are highest for FeTi and lowest for NiTi. This indicates that both these properties are directly proportional to ultrasonic velocities and in turn ultrasonic velocities and ultrasonic Grüneisen parameters depend on the elastic constants. The elastic constants are generated with the help of two basic parameters nearest neighbor distance and hardness parameter. Hence these two parameters are playing very important role in present investigation.

Therefore, the present method has the potential to intensify the prospects of preceding formulism based on elastic theory of materials to predict the occurrence of phase transitions, thermal elastic behavior, electron-phonon interaction and phonon-phonon interaction mechanism.

5. Acknowledgement

We extend special thanks to Mr. Ajit Kumar Maddheshiya for meticulously reading the manuscript and making the figures carefully.

6. References

[1] Zhang L, Chen H, Wang Z, Ma L, Tang P. Theoretical predictions of structure, mechanics, dislocation and electronics properties of FeTi alloy at high pressure. Metals. 2023;13(9):1547.
[2] Wollmershauser JA, Neil CJ, Agnew SR. Mechanisms of ductility in CoTi and CoZr B2 Intermetallics. Metall Mater Trans A. 2010;41:1217-29.
[3] Kaneno Y, Takasugi T, Hanada S. Tensile property and fracture behaviour of hot-rolled CoTi intermetallic compound. Mater Sci Eng A. 2001;302(2):215-21.
[4] Koroteev YM, Lipnitskii AG, Chulkov EV, Silkin VM. The (110) surface electronic structure of FeTi, CoTi and NiTi. Surf Sci. 2002;507-510:199-206.
[5] Bihlmayer G, Eibler R, Neckel A. Elastic properties of B2-NiTi and B2-PdTi. Phys Rev B. 1994;50(18):13113-7.
[6] Brill TM, Mittelbach S, Assmus W, Mullner M, Luthi B. Elastic properties of NiTi. J Phys: Condens Matter. 1991;3:9621.
[7] Haskins JB, Lawson JW. Finite temperature properties of NiTi from first principles simulations: structure, mechanics and thermodynamics. J Appl Phys. 2017;121(20):205103.
[8] Zhu LF, Friák M, Udyansky A, Ma D, Schlieter A, Kühn U, et al. Ab initio-based study of finite-temperature structural, elastic and thermodynamic properties of FeTi. Intermetallics. 2014;45:11-7.
[9] Yu F, Liu Y. First-principles calculations of structural, mechanical and electronic properties of the B2-phase NiTi shape-memory alloy under high pressure. Computation. 2019;7(4):57.
[10] Matsushita M, Tajima I, Abe M, Tokuyama H. Experimental study of porosity and effective thermal conductivity in packed bed of nano-structured FeTi for usage in hydrogen storage tanks. Int J Hydrogen Energy. 2019;44(41):23239-48.
[11] Cheng D, Zhao S, Wang S, Ye H. First-principles study of elastic properties and electronic structure of NiTi, CoTi and FeTi. Philos Mag A. 2001;81(6):1625-32.
[12] Lu W, Li C, Yi J, Li K. Stability and elastic properties of B2 CoX (X= Ti, Zr and Hf) intermetallic compounds as a function of pressure. Philos Mag. 2018;98(3):203-18.

[13] Zadorozhnyy VY, Klyamkin SN, Kaloshkin SD, Skakov YA. Production of intermetallic compound of FeTi by means of mechanical-chemical synthesis and its interaction with hydrogen. Inorg Mater Appl Res. 2010;1:41-5.
[14] Tessier P, Schulz R, Ström-Olsen JO. Elastic stress in composite FeTi hydrogen storage materials. J Mater Res. 1998;13(6):1538-47.
[15] Benyelloul K, Bouhadda Y, Bououdina M, Faraoun HI, Aourag H, Seddik L. The effect of hydrogen on the mechanical properties of FeTi for hydrogen storage applications. Int J Hydrogen Energy. 2014;39(24):12667-75.
[16] Padhee SP, Roy A, Pati S. Mechanical insights into efficient reversible hydrogen storage in ferrotitanium. Int J Hydrogen Energy. 2021;46(1):906-21.
[17] Born M, Mayer JE. Zur Crittertheorie der Ionenkristalle. Zeitschrift für Physik. 1932; 75:1-18. (In German)
[18] Brugger K. Thermodynamic definition of higher order coefficients. Phys Rev. 1964;133(6A):A1611-2.
[19] Ghate PB. Third order elastic constants of alkali halide crystals. Phys Rev. 1965;139(5A):A1666-74.
[20] Yadav RR, Pandey DK. Size dependent acoustical properties of bcc metal. Acta Phys Pol A. 2005;107(6):933-46.
[21] Bala J, Singh SP, Verma AK, Singh DK, Singh D. Elastic, mechanical and ultrasonic studies of boron monopnictides in two different structural phases. Indian J Phys. 2022;96:3191-200.
[22] Singh D, Pandey DK. Ultrasonic investigation in intermetallics. Pramana. 2009;72(2):389-98.
[23] Morelli DT, Slack GA. High lattice thermal conductivity solids. In: Shinde SL, Goela JS, editors. High Thermal Conductivity Materials. New York: Springer; 2006. p. 37-68.
[24] Mason WP. Effect of impurities phonons process on the ultrasonic attenuation of germanium crystal quartz and silicon. In: Mason WP, editor. Physical Acoustics: Principle and Methods, Vol. 3, Part B. New York: Academic press; 1965. p. 235-86.
[25] Gray DE. American Institute of Physics Handbook. 3rd ed. New York: Mc Graw–Hill; 1972.
[26] Acharya N, Fatima B, Chouhan SS, Sanyal SP. First principles study on structural, elastic and thermal properties of equiatomic MTi (M=Fe, Co, Ni). Chem Mater Res. 2013;3(8):22-30.
[27] Tosi MP. Cohesion of ionic solids in the Born model. Solid State Phys. 1964;16:1-120.
[28] Born M, Huang K. Dynamical theory of crystal lattices. Oxford; Clarendon Press; 1954.
[29] Cousin CSG. New relations between elastic constants of different orders under central force interactions. J Phys C Solid State Phys. 1971;4:1117.
[30] Tripathi S, Agrawal R, Singh D. Nonlinear elastic, ultrasonic and thermophysical properties of lead telluride. Int J Thermophys. 2019;40:78.
[31] Pugh SF. XCII. Relations between the elastic moduli and the plastic properties of polycrystalline pure metals. Lond Edinb Dublin Philos Mag J Sci. 1954;45:823-43.
[32] Watt JP. Elastic properties of polycrystalline minerals: comparison of theory and experiment. Phy Chem Minerals. 1988;15:579-87.
[33] Terada Y, Nakata J, Mohri T, Suzuki T. A method for seeking high thermal conductivity compounds. Intermetallics. 1998;6(6):479-85.
[34] Yadav RR, Singh D. Ultrasonic attenuation in lanthanum monochalcogenides. J Phys Soc Jpn. 2001;70(6):1825-32.